J. Fluid Mech. (1979), *vol.* 92, *part* 3, *pp.* 401–419
Printed in Great Britain

The low-shear limit of the effective viscosity of a solution of charged macromolecules

By WILLIAM B. RUSSEL

Department of Chemical Engineering, Princeton University,
Princeton, New Jersey 08540

(Received 11 April 1978)

The effect of pair interactions between charged macromolecules on the bulk stress is calculated for the Newtonian low-shear limit. Electrostatic force laws are derived for molecular conformations corresponding to the limits of weak and strong intramolecular repulsions and used to determine the equilibrium pair distribution function and the perturbation due to the flow. Intramolecular and near-field intermolecular hydrodynamic interactions are neglected as appropriate for so-called free draining macromolecules. The resulting bulk stress contains separate contributions from the far-field hydrodynamic interactions and the electrostatic forces. The coefficient of the $O(c^2)$ term in the viscosity which equals 0·4 in the purely hydrodynamic limit is predicted to increase dramatically with decreasing ionic strength for charged macromolecules in agreement with experimental data in the literature.

1. Introduction

Polymer solutions are non-ideal in both their thermodynamic and their mechanical properties. Typical of the thermodynamical effects are large second virial coefficients which vary with the solution chemistry (e.g. Yamakawa 1971). On the mechanical side shear-rate dependent viscosities and elastic effects such as normal stress differences in shear flows and large extensional viscosities are common (e.g. Bird *et al.* 1977; Schowalter 1978). These phenomena arise from the influence of intermolecular forces and viscous stresses on the microstructure of the macromolecular solution. Unlike normal solutions with molecular dimensions smaller than 100 Å in which only strong, short-range forces can compete with the intense thermal motion in determining the liquid structure, the larger macromolecular dimensions (10^2–10^4 Å) permit viscous forces and intermolecular interactions with length scales on the order of a micron to influence both the conformation and spatial distribution of polymer molecules. Since this 'macromolecular structure' controls the bulk thermodynamic and mechanical properties the appearance of non-idealities is easy to understand qualitatively but difficult to quantify except in the dilute limit.

Here the shear viscosity normalized with the solvent viscosity μ_0 can be expanded in powers of the weight concentration c as

$$\mu/\mu_0 = 1 + [\eta]c + k[\eta]^2c^2 + \dots \ .$$

The coefficient $[\eta]$ generally known as the intrinsic viscosity reflects the spatial extent of an isolated macromolecule and the Huggins' coefficient k the effect of pair interactions. For uncharged polymers $k \sim 0{\cdot}3$–$1{\cdot}0$, making the c^2 term insignificant until

0022-1120/79/4235-6230 $02.00

$[\eta]c \sim O(1)$ and uninteresting even then since k changes little with molecular weight or shear rate. In concentrated solutions changes in molecular conformation also seem to negate other interaction effects in the absence of physical entanglements. For this reason the dynamics of individual macromolecules have been probed extensively for insight into the rheology of moderately concentrated polymer solutions (e.g. Williams 1975; Bird *et al.* 1977).

Solutions of charged polymers, commonly known as polyelectrolytes, are significantly more non-ideal because of their sensitivity to the ionic strength of the free electrolyte and the dissociation of the fixed charges. Intramolecular electrostatic interactions tend to expand the macromolecule and therefore increase $[\eta]$ while intermolecular interactions affect k. For a highly charged macromolecule both $[\eta]$ and k can increase by an order of magnitude from high to low ionic strengths (Moan & Wolff 1974; Pals & Hermans 1952). As a result interactions influence the viscosity at lower concentrations

$$[\eta]c \gtrsim \frac{1}{k}$$

and both $[\eta]$ and k become more shear-rate dependent. More concentrated solutions of technical importance in tertiary oil recovery processes, for example, display this same sensitivity to electrochemical environment and shear rate (Mungan 1972). A study of dilute solutions intended to elucidate the complex relationship between bulk rheology and molecular parameters at these higher concentrations therefore must include pair interactions at least.

The $O(c)$ electrostatic influence, i.e. the enhancement in $[\eta]$, can be estimated from existing theories for the dynamics of isolated polymer molecules and the expansion engendered by intramolecular forces of non-electrostatic origin (Yamakawa 1971). More accurate predictions may soon be available from a new approach proposed by Edwards (1965) and developed further by de Gennes (1969) and others. Limited theoretical results and the scarcity of data on well-characterized solutions currently makes evaluation difficult, however.

Here we concentrate on the pair interaction problem, one which has surfaced occasionally in the polymer literature but until recently had not been solved even for uncharged macromolecules. Analyses have focused on the limiting cases of negligible and dominant intramolecular hydrodynamic interactions, generally termed free-draining and non-draining, respectively. The problem lies in the slow decay of the intermolecular hydrodynamic interactions which renders straightforward calculations non-unique. Saito (1950) first correctly circumvented the mathematical difficulty through physical reasoning to obtain $k = 0{\cdot}40$ in the absence of near-field hydrodynamic interactions. Recently Felderhof (1976) rigorously substantiated this result. Although neither author stated so explicitly this represents the correct limit for free-draining macromolecules under thermodynamically ideal conditions, i.e. no net intermolecular forces. Peterson & Fixman (1963) handled the non-convergent integrals correctly in the non-draining limit to find $k = 0{\cdot}69$ for non-penetrating spheres and $k = 0{\cdot}88$ for interpenetrating spheres but employed only approximate hydrodynamics and failed to appreciate the stresses generated directly by Brownian forces. By taking the dilute limit of their mean-field theory for concentrated polymer solutions Freed & Edwards (1975) obtained $k = 0{\cdot}75$ in the non-draining limit for a Gaussian chain

molecule without intermolecular forces; however, near-field hydrodynamic interactions and Brownian forces again appear to have been omitted. Only recently Batchelor (Batchelor & Green 1972; Batchelor 1977) rigorously accounted for the non-convergent integrals, the hydrodynamic interactions and the Brownian forces to obtain $k = 0{\cdot}99$ for non-draining and non-penetrating spheres.

This paper applies Batchelor's approach to pair interactions between free-draining macromolecules subject to Brownian motion and intermolecular electrostatic forces. The thermodynamically ideal state assumed in the absence of electrostatic forces permits complete interpenetration of the macromolecules and produces $k = 0{\cdot}40$ in accord with Saito and Felderhof. Only in the limit of strong repulsions do we obtain the hard sphere excluded volume considered by Batchelor and Fixman (1965), but the corresponding Huggins' coefficient substantially exceeds their values because of the electrostatic contribution to the stress.

A similar concern with the role of intermolecular forces in concentrated polymer solutions led Williams (1966, 1967) to develop an approximate theory for pair interactions. He used existing formulations for the bulk stress (Fixman 1965), the intermolecular potential (Flory 1945), and the pair distribution function (Kirkwood, Buff & Green 1949) which resemble ours, but evaluated them through approximations which are invalid in the dilute limit. Non-Newtonian effects were predicted as a consequence of molecular deformation due to shear altering the intermolecular forces.

This paper opens with a discussion of an isolated free-draining macromolecule to explain the uncertainty in the intramolecular segment density and motivate the choice of Gaussian and uniform distributions for the pair interaction analysis. The necessary hydrodynamic results for both are obtained quite simply and then used to derive the bulk stresses complete with contributions from viscous, Brownian, and other intermolecular forces. In a manner reminiscent of the Flory (1945) and Flory & Krigbaum (1950) theories for solution thermodynamics electrostatic force laws are developed and incorporated into a pair conservation equation of standard form. From that point we restrict the analysis to the low-shear or strong Brownian motion limit permitting an expansion of the pair density as the equilibrium result plus a small perturbation due to flow. Solutions for the latter in several limiting cases produce bulk stresses and Huggins' coefficients which demonstrate the dramatic effect of electrostatic forces and are conveniently insensitive to the form chosen for the segment distribution. Finally, comparison of the predictions with the data of Pals & Hermans (1952) shows reasonable agreement. The existing discrepancies appear to arise from non-Newtonian effects at the finite experimental shear rates.

2. Conformation of charged macromolecules

A model for the internal structure and the dynamics of individual macromolecules is essential to the analysis of pair interactions. For uncharged polymers many sophisticated theories based on statistical descriptions of the polymer chain have followed the random flight model originally presented by Kuhn and by Guth & Mark in the 1930s. Calculations including detailed segment-segment interactions have predicted with some success thermodynamic properties such as osmotic pressure as well as transport properties including the intrinsic viscosity and the friction coefficient (Yamakawa 1971). Most of the dynamical theories (Kirkwood & Riseman 1948;

Rouse 1953; Zimm 1956) pertain to thermodynamically ideal polymers with no excluded volume for which the equilibrium conformation is a Gaussian coil.

With polyelectrolytes non-idealities arise primarily from the interaction of fixed charges along the polymer backbone as mediated by low molecular weight salts in solution. High ionic strengths effectively shield the fixed charges allowing the macromolecule to relax to a random, or Gaussian, coil, but the removal of electrolyte increases the repulsion between segments causing a flexible macromolecule to expand. Attempts to predict the expansion factor began with Hermans & Overbeek (1948), who assumed the Gaussian form to be preserved but determined the radius of gyration by minimizing the sum of the electrostatic and the entropic free energies calculated from a smoothed segment density. Recently Edwards (1965) and de Gennes (1969) have developed 'self-consistent' approaches along the same lines which would determine the segment distribution as part of the solution. To date only asymptotic results for small and large expansions are available (Richmond 1973; de Gennes, Pincus & Velasco 1976; Bailey 1977).

In the absence of a general theory for polyelectrolyte conformation, we have chosen two forms for the segment distribution felt to characterize the limiting cases of strong and weak electrostatic effects and will treat the radius of gyration r_g as an independent parameter. The ideal limit at high ionic strengths or low charge densities will be represented by the Gaussian segment density

$$p(r) = \left(\frac{3}{2\pi r_g^2}\right)^{\frac{3}{2}} \exp\left(-\frac{3r^2}{2r_g^2}\right), \tag{1}$$

where

$$r_g^2 = \int r^2 p(\mathbf{r})\, d^3\mathbf{r} \tag{2}$$

is the mean squared radius of gyration. The other limit of dominant electrostatic repulsions at low ionic strengths or high charge densities should produce a more uniform spacing between segments approximated by

$$p(r) = \frac{3}{4\pi a^3} \begin{cases} 1 & \text{for } r < a \\ 0 & \text{for } r > a \end{cases} \tag{3}$$

with $r_g^2 = \frac{3}{5}a^2$. In the following sections the hydrodynamics and electrostatics of these models will be reviewed.

3. The hydrodynamics of free-draining macromolecules

In this analysis of intermolecular interactions we neglect intramolecular hydrodynamic interactions and molecular deformation, which should be reasonable for somewhat expanded polyelectrolytes in weak flows.

Under these conditions an individual bead, or friction centre, at position $\mathbf{x}_i$ relative to the centre of mass has velocity

$$\mathbf{U}_0 + \boldsymbol{\omega}_0 \times \mathbf{x}_i,$$

determined by the translation $\mathbf{U}_0$ and rotation $\boldsymbol{\omega}_0$ of the rigid macromolecule, and experiences the undisturbed velocity of the fluid $\mathbf{u}_\infty(\mathbf{x}_i)$. The difference between these two velocities produces a viscous force on the bead

$$\mathbf{F}_i = f_0(\mathbf{u}_\infty(\mathbf{x}_i) - \mathbf{U}_0 - \boldsymbol{\omega}_0 \times \mathbf{x}_i), \tag{4}$$

where f_0 is the friction coefficient of the bead. The opposing force exerted by the bead on the fluid generates a disturbance velocity field which affects the bulk properties of the solution.

For a macromolecule moving through a quiescent fluid with $\mathbf{u}_\infty = \boldsymbol{\omega}_0 = 0$ the total force follows as the sum of $\mathbf{F}_i$ over all beads or equivalently

$$\begin{aligned} \mathbf{F} &= -f_0 \mathbf{U}_0 N \int p(\mathbf{r})\, d^3\mathbf{r} \\ &= -f_0 N \mathbf{U}_0 \end{aligned} \tag{5}$$

since the segment density $p(\mathbf{r})$ is normalized. Thus without hydrodynamic interactions the molecular friction coefficient is simply the sum of the bead coefficients.

One can derive the viscosity of a dilute solution in a similar fashion by noting that each segment contributes to the bulk stress as

$$\boldsymbol{\Sigma}(\mathbf{x}_i) = \int \boldsymbol{\sigma}(\mathbf{x} - \mathbf{x}_i)\, d^3\mathbf{x} = \mathbf{x}_i \mathbf{F}_i, \tag{6}$$

where $\boldsymbol{\sigma}$ is the stress field in the fluid generated by the point force $\mathbf{F}_i$. For a homogeneous shear flow

$$\mathbf{u}_\infty(\mathbf{x}_i) = \mathbf{E} . \mathbf{x}_i + \boldsymbol{\omega}_0 \times \mathbf{x}_i, \quad \mathbf{U}_0 = 0 \tag{7}$$

where $\mathbf{E}$ is the symmetric rate of strain tensor far from the macromolecule

$$\begin{aligned} \boldsymbol{\Sigma}^p &= nN \int \boldsymbol{\Sigma}(\mathbf{r})\, p(\mathbf{r})\, d^3\mathbf{r} \\ &= \tfrac{1}{3} n f_0 N r_g^2 \mathbf{E} + O(n^2) \end{aligned} \tag{8}$$

with n the number density of macromolecules. The conventional form in terms of the mass concentration $c = M_w n / N_A$

$$\boldsymbol{\Sigma}^p = 2\mu_0 [\eta]\, c \mathbf{E} \tag{9}$$

determines the intrinsic viscosity

$$[\eta] = \tfrac{1}{6} \frac{N_A f_0 N}{\mu_0 M_w} r_g^2, \tag{10}$$

where N_A is Avogadro's number and M_w the molecular weight. Thus for free-draining macromolecules the conformation only enters through the dependence of r_g^2 on molecular parameters; for example substitution of $r_g^2 = \frac{1}{6} N l^2$ for a Gaussian coil with statistical segments of length l transforms (10) into Rouse's (1953) result while $r_g^2 = \frac{3}{5} a^2$ for a uniform segment density reproduces the porous sphere result of Debye & Bueche (1948) and Brinkman (1947).

The neglect of hydrodynamic interactions within the macromolecule in the free-draining limit necessitates the neglect of near-field interactions between macromolecules. Two molecules with vector separation $\mathbf{r}$ subject to equal but opposite forces $\mathbf{F}$ and $-\mathbf{F}$ and imbedded in the flow field (7) therefore have relative velocity

$$\mathbf{U} = \frac{2}{N f_0} \mathbf{F} + \mathbf{E} . \mathbf{r} + \boldsymbol{\omega}_0 \times \mathbf{r}. \tag{11}$$

Exceptions to this statement arise only in the calculation of concentration-dependent bulk properties from local pair interactions as shown by Felderhof (1976).

4. Bulk stress in dilute suspensions with Brownian motion

Each of the forces active at the microscopic level in a colloidal suspension or a polymer solution, e.g. viscous, Brownian, and electrostatic, may contribute to the bulk stress. Batchelor has derived the general form of the viscous and Brownian contributions for interacting spheres (Batchelor 1970; Batchelor & Green 1972; Batchelor 1977). An extension of the same approach to include electrostatic forces between the spheres (Russel 1976) produced a dipole form for the bulk stress in the absence of hydrodynamic interactions in agreement with that for non-interacting dumbbells (Bird *et al.* 1977). In the following these results are applied to interactions between free-draining macromolecules.

The bulk stress in an electrolyte solution is the volume average of the viscous and Maxwell stresses plus the momentum flux tensor, i.e.

$$\boldsymbol{\Sigma} = \frac{1}{V}\int_V (\boldsymbol{\sigma} + \mathbf{m} - \rho\mathbf{u}\mathbf{u})\, dV = -nkT\boldsymbol{\delta} + \frac{1}{V}\int_V (\boldsymbol{\sigma} + \mathbf{m})\, dV, \tag{12}$$

where $\mathbf{m} = \epsilon(\nabla\psi\nabla\psi - \frac{1}{2}\boldsymbol{\delta}\nabla\psi.\nabla\psi)$. Because of the low Reynolds number of the steady state motion the momentum flux only contributes the initial isotropic term arising from the kinetic energy of the individual macromolecules (Bird *et al.* 1977).

A more meaningful form for the bulk stress is obtained by isolating the contribution from the pure solvent and following Batchelor's (1970) manipulations to obtain

$$\boldsymbol{\Sigma} = -p_0\boldsymbol{\delta} + 2\mu_0\mathbf{E} + \boldsymbol{\Sigma}^p, \tag{13}$$

where the particle stress in the absence of near-field hydrodynamic interactions is

$$\boldsymbol{\Sigma}^p = -nkT\boldsymbol{\delta} + \boldsymbol{\Sigma}^p_{\text{hyd}} - \frac{1}{V}\sum_{n=1}^{\infty} \mathbf{x}_n\mathbf{F}_n. \tag{14}$$

Here the contribution of the intermolecular forces $\mathbf{F}_n$ has been isolated in the final term leaving $\boldsymbol{\Sigma}^p_{\text{hyd}}$ as the viscous stress generated by the imposed shear field.

Batchelor & Green (1972) and Felderhof (1976) have demonstrated that the hydrodynamic particle stress in the absence of near-field interactions is

$$\boldsymbol{\Sigma}^p_{\text{hyd}} = 5n\alpha\mu_0\mathbf{E}(1 + \alpha n). \tag{15}$$

For free-draining macromolecules

$$\alpha = \tfrac{2}{5}[\eta]\, M_w/N_A \tag{16}$$

so that

$$\boldsymbol{\Sigma}^p = -nkT\boldsymbol{\delta} + 2\mu_0\mathbf{E}[\eta]\, c\,(1 + \tfrac{2}{5}[\eta]\, c) - \frac{1}{V}\sum_{n=1}^{N} \mathbf{x}_n\mathbf{F}_n. \tag{17}$$

In the absence of intermolecular forces (17) predicts a Huggins' coefficient of 0·40 for free-draining macromolecules independent of the segment distribution, molecular weight, and radius of gyration as found by Saito (1950) and Felderhof (1976).

For pair interactions the last term can be written in terms of the probability density $P(\mathbf{r})$ for a second particle at position $\mathbf{r}$ with respect to the test particle

$$\boldsymbol{\Sigma}^p_{\text{inter}} = -\tfrac{1}{2}n\int \mathbf{r}\mathbf{F}P(\mathbf{r})\, d^3\mathbf{r}. \tag{18}$$

The factor of $\frac{1}{2}$ appears because N particles in volume V produce only $\frac{1}{2}N$ pairs. Fixman (1965) derived (18) but neglected the $O(c^2)$ hydrodynamic interaction.

Results for two related problems support these arguments. Bird and co-workers have developed the kinetic theory of elastic dumbbells as a model for macromolecules in solution (e.g. Bird *et al.* 1977). The two beads are generally taken as friction points, i.e. no volume, so that $\alpha \equiv 0$ but forces are transmitted between the beads by the connector. Then with $\mathbf{F}_n = \mathbf{F}_n^{\text{spring}}$ and $P(\mathbf{r}) = \delta(\mathbf{r} - \mathbf{r}_0)$, the above result agrees with the stress derived from kinetic theory,

$$\boldsymbol{\Sigma} = -nkT\boldsymbol{\delta} - \tfrac{1}{2}n\langle \mathbf{r}_0 \mathbf{F}^{sp} \rangle, \tag{19}$$

where $\mathbf{r}_0$ is the vector separation of the beads, $\frac{1}{2}n$ is the number of dumbbells and $\langle\ \rangle$ denotes the configurational average. Similarly the osmotic pressure in a dilute polymer solution, derived from the chemical potential using MacMillan–Mayer theory (Yamakawa 1971)

$$\pi = nkT + \tfrac{1}{6}n^2\langle \mathbf{r} . \mathbf{F} \rangle, \tag{20}$$

corresponds to the pressure predicted by (17).

Experiments with uncharged polymers in ideal or theta solvents, i.e. without thermodynamic interactions, generally find $0{\cdot}4 \leqslant k \leqslant 1{\cdot}0$, possibly indicating weak hydrodynamic interactions (Berry 1967). As will be shown in the following sections, polyelectrolyte solutions often have much larger Huggins' coefficients reflecting strong intermolecular electrostatic forces.

5. Electrostatic force laws

Analyses of equilibrium double layers, i.e. the distribution of free ions around a fixed charge in the absence of fluid motion, generally begin with the Poisson–Boltzmann equation for the potential ψ

$$\nabla^2\psi = -\frac{e}{\epsilon}\sum_i z_i n_i^{\infty} \exp\left(-\frac{ez_i\psi}{kT}\right). \tag{21}$$

Here e is the electronic charge, ϵ the dielectric constant, z_i the ionic valence, n_i^{∞} the ion concentration in the bulk fluid, and kT the Boltzmann temperature. The right-hand side comprises the net charge density in the fluid, obtained by summing ez_i times the ion concentrations. The Boltzmann distribution of the latter shown in (21) is a result of integrating the individual conservation equations. The assumptions implicit in (21) have been critically examined by Kirkwood (1934) and Bell & Levine (1966). The most notable are the treatment of free ions as point charges, the smoothing of the space charge into a uniform distribution, and the assumption of a constant dielectric constant for the fluid. Difficulties do arise, particularly at high ionic strengths, but tractable alternatives have yet to appear.

In this section electrostatic force laws for interacting charged macromolecules are derived on the basis of three additional assumptions.

(i) The physically excluded volume occupied by the polymer backbone can be neglected.

(ii) A smoothed density for the fixed charges can be substituted into the Poisson–Boltzmann equation in place of discrete locations along the backbone.

(iii) The electrostatic potential in the fluid is sufficiently small for the Poisson–Boltzmann equation to be linearized.

While not original with this work these assumptions will be discussed in some detail.

For a flexible macromolecule in an ideal, or theta, solvent the radius of gyration

$$r_g^2 = \tfrac{1}{6}Nl^2 \tag{22}$$

depends only on the number N and the length l of the statistical segments. If each segment has radius $a \lesssim l$ the volume fraction of polymer within the coil is approximately

$$Na^2l/r_g^3 \sim N^{-\frac{1}{2}}(a/l)^2 \ll 1. \tag{23}$$

Thus the point charge approximation should be valid except when attractive intramolecular forces collapse the coil into a globular form.

The restriction to small [or at most $O(1)$] dimensionless potentials $e\psi/kT$ is both mathematically necessary and physically reasonable for polyelectrolytes. In the vicinity of the polymer backbone where the potential is largest the fixed charges resemble a line charge with linear density β. If $e|z|\beta/\epsilon kT$ (with $|z|$ the counter-ion valence) exceeds unity the intense electric field causes counterions to 'condense' on the excess fixed charges, effectively neutralizing them (see e.g. Manning 1974). Thus the corresponding potential

$$e\psi/kT \sim e\beta/\epsilon kT \tag{24}$$

cannot exceed one anywhere.

With these assumptions the potential around a single polyelectrolyte molecule centred at $r = 0$ is determined by

$$\nabla^2\psi = \kappa^2\psi - \frac{Q}{\epsilon}\,p(r) \tag{25}$$

with $$\psi \to 0 \quad \text{as} \quad r \to \infty \quad \text{and} \quad \lim_{r\to 0} r^2 \frac{d\psi}{dr} = 0.$$

$p(r)$ is the normalized segment density and Q the total charge. Rather than solving (25) for arbitrary $r_g\kappa$ we merely note two limiting cases,

$$\psi = \frac{Q}{\epsilon}\left\{\frac{1}{r}\int_0^r x^2 p(x)\,dx + \int_r^\infty x p(r)\,dx\right\} \quad \text{for} \quad r_g\kappa \ll 1 \tag{26}$$

and

$$\psi = \frac{Q}{\epsilon\kappa^2}\,p(r) \quad \text{for} \quad r_g\kappa \gg 1. \tag{27}$$

Only (27) will be needed below because the expansion of flexible polyelectrolytes with decreasing ionic strength generally maintains $r_g\kappa \gg 1$.

Interactions between two charged macromolecules can be described by superimposing the individual potentials; because of the point charge approximation the equation and boundary conditions are still satisfied. Likewise the potential energy of a second macromolecule with segment density $p_2(\mathbf{r})$ residing in the potential field $\psi_1(\mathbf{r})$ of the first equals the sum of the energy of its fixed charges or

$$\begin{aligned} V(r_{12}) &= \int Q p_2(\mathbf{r})\,\psi_1(\mathbf{r})\,d^3\mathbf{r} \\ &= \frac{Q^2}{\epsilon\kappa^2}\int p_1(\mathbf{r})\,p_2(\mathbf{r})\,d^3\mathbf{r} \quad \text{for} \quad r_g\kappa \gg 1. \end{aligned} \tag{28}$$

Clearly for $r_g\kappa \gg 1$ the molecules must overlap to interact. The integral takes a more convenient form in the cylindrical co-ordinates of figure 1,

$$V(r_{12}) = 2\pi\frac{Q^2}{\epsilon\kappa^2}\int_0^\infty\int_{-\infty}^\infty \rho p(r_1)\,p(r_2)\,dz\,d\rho \tag{29}$$

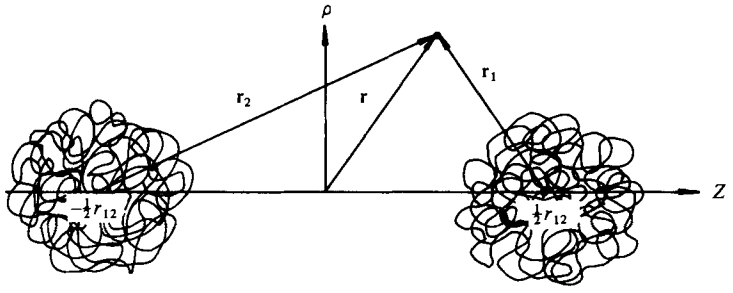

FIGURE 1. Cylindrical co-ordinate system for pair interactions.

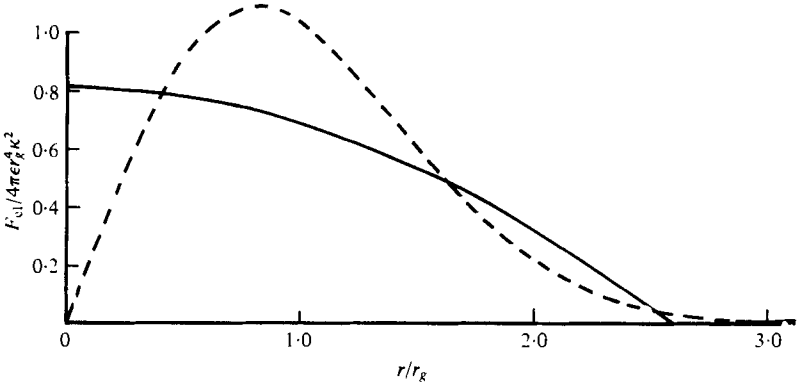

FIGURE 2. Electrostatic forces as a function of separation for uniform (——) and Gaussian (– – –) segment densities.

with

$$r_1^2 = \rho^2 + (z - \tfrac{1}{2}r_{12})^2, \quad r_2^2 = \rho^2 + (z + \tfrac{1}{2}r_{12})^2.$$

The results for the intermolecular potential and the corresponding force for the two segment densities follow.

(*a*) Gaussian:

$$V(r_{12}) = \frac{1}{8}\left(\frac{3}{\pi}\right)^{\frac{3}{2}} \frac{Q^2}{\epsilon r_g^3 \kappa^2} \exp\left(-\frac{3r_{12}^2}{4r_g^2}\right),$$

$$F_{el}(r_{12}) = -\frac{dV}{dr_{12}} = \frac{3}{16}\left(\frac{3}{\pi}\right)^{\frac{3}{2}} \frac{Q^2}{\epsilon r_g^4 \kappa^2} \frac{r_{12}}{r_g} \exp\left(-\frac{3r_{12}^2}{4r_g^2}\right). \tag{30}$$

(*b*) Uniform:

$$V(r_{12}) = \frac{3}{4\pi} \frac{Q^2}{\epsilon a^3 \kappa^2}\left(1 - \frac{3r_{12}}{4a} + \frac{r_{12}^3}{16a^3}\right),$$

$$F_{el}(r_{12}) = \frac{9}{16\pi} \frac{Q^2}{\epsilon a^4 \kappa^2}\left(1 - \frac{r_{12}^2}{4a^2}\right), \tag{31}$$

for $r_{12} < 2a$.

With $r_g^2 = \frac{3}{5}a^2$ the latter becomes

$$F_{el}(r_{12}) = \frac{81}{400\pi} \frac{Q^2}{\epsilon r_g^4 \kappa^2}\left(1 - \frac{3r_{12}^2}{20r_g^2}\right) \tag{32}$$

which is compared with (30) in figure 2. The two forces have similar ranges and magnitudes but markedly different forms; the effect on bulk properties such as viscosity and osmotic pressure will be calculated in the following sections.

6. Weak-flow limit of the pair conservation equation

The weak-flow assumption which permitted the neglect of macromolecular deformation also simplifies the description of pair interactions. Below we formulate the conservation equation for the pair density $P(\mathbf{r})$, which specifies the probability of finding a second molecule at $\mathbf{x}+\mathbf{r}$ given a test molecule at $\mathbf{x}$, and then expand in a regular perturbation about the equilibrium pair density $P_0(r)$ to calculate the first-order effect of flow. If non-hydrodynamic forces affect the pair distribution, this small perturbation contributes to the bulk stress at the same order as the viscous stress corresponding to the equilibrium configuration.

The conservation equation for the pair density in configuration space $\mathbf{r}$ is

$$\partial P/\partial t + \nabla . P\mathbf{U} = 0. \tag{33}$$

with $\mathbf{U}$ from (11). For a thermodynamically ideal solution in the absence of charges, only Brownian and electrostatic forces need be considered so

$$\mathbf{F} = F_{\mathrm{el}}\mathbf{r}/r - kT\nabla \ln P. \tag{34}$$

Then the scaled conservation equation for a homogeneous shear flow is

$$\partial P/\partial \tau + \Gamma(\bar{\mathbf{E}}+\bar{\mathbf{\Omega}}).\mathbf{R}.\nabla P + \alpha\nabla.(Pf_{\mathrm{el}}\mathbf{R}/R) = \nabla^2 P, \tag{35}$$

where

$$\Gamma = \frac{Nf_0}{2kT} r_g^2 (\mathbf{E}:\mathbf{E})^{\frac{1}{2}}, \quad \alpha = \frac{Q^2}{4\pi\epsilon r_g^3 \kappa^2 kT},$$

$$f_{\mathrm{el}} = F_{\mathrm{el}} \frac{4\pi\epsilon r_g^4 \kappa^2}{Q^2}, \quad \tau = \frac{2kT}{Nf_0 r_g^2} t, \quad \mathbf{R} = \frac{\mathbf{r}}{r_g},$$

and $\bar{\mathbf{E}}$ and $\bar{\mathbf{\Omega}}$ are the dimensionless rate-of-strain and vorticity tensors, respectively. The boundary conditions

$$\left.\begin{aligned} R^2 \partial P/\partial R &\to 0 \quad \text{as} \quad R \to 0, \\ P &\to n \quad \text{as} \quad R \to \infty \end{aligned}\right\} \tag{36}$$

specify a random bulk solution dominated by Brownian motion and thereby exclude the possibility of long-range order.

Weak flows can now be defined by $\Gamma \ll 1$ and the regular expansion

$$P(\mathbf{R}) = P_0(R)(1 + \Gamma g(R)\mathbf{R}.\bar{\mathbf{E}}.\mathbf{R}/R^2) \tag{37}$$

used to decompose (35) into an $O(1)$ equation for P_0 and an $O(\Gamma)$ for g. At steady state the former,

$$\alpha\nabla . P_0 f_{\mathrm{el}} \frac{\mathbf{R}}{R} = \nabla^2 P_0$$

with

$$\begin{aligned} R^2 dP_0/dR &\to 0 \quad \text{as} \quad R \to 0, \\ P_0 &\to n \quad \text{as} \quad R \to \infty, \end{aligned} \tag{38}$$

has solution

$$P_0(R) = n \exp\left\{-\alpha \int_R^\infty f_{\mathrm{el}}\, dR\right\}. \tag{39}$$

Without an electrical force $P_0(R) \equiv n$ and the macromolecules freely interpenetrate, but $f_{\mathrm{el}} \neq 0$ generates an excluded volume which for large α can be approximated from

the radius at which the exponent in (39) becomes $O(1)$; this leads to

$$\tfrac{3}{3}\tfrac{2}{3}\pi r_g^3 \times \begin{cases} (\ln\alpha/3)^{\frac{3}{2}} & \text{(Gaussian)} \\ (\frac{5}{3})^{\frac{3}{2}} & \text{(uniform).} \end{cases}$$

The latter represents two impenetrable spheres of radius $a = (\frac{5}{3})^{\frac{1}{2}} r_g$.

The $O(\Gamma)$ ordinary differential equation for $g(R)$ is

$$\frac{1}{R^2}\frac{d}{dR} R^2 \frac{dg}{dR} + \alpha f_{\mathrm{el}} \frac{dg}{dR} - \frac{6}{R^2} g = \alpha f_{\mathrm{el}} R \tag{40}$$

with
$$dg/dR = 0 \quad \text{at} \quad R = 0,$$
$$g \to 0 \quad \text{as} \quad R \to \infty.$$

The forcing term on the right-hand side is the deformation of the equilibrium distribution by the weak flow. In the following sections solutions to (40) will be presented with the corresponding particle stresses for Gaussian and uniform segment densities.

Gaussian segment density

For the Gaussian segment density (1) characteristic of an ideal random coil the exponential dependence of the electrostatic force law (30) renders the transformed pair conservation equation (40) rather tedious to solve analytically with a power series in R so only the asymptotic results for small and large α will be presented. In fact the leading terms in these asymptotic expansions provide a surprisingly clear indication of the particle stress and, hence, the Huggins coefficient over the entire range of α.

Electrostatic forces which are weak relative to Brownian motion, i.e. $\alpha \ll 1$, make the equilibrium distribution only slightly non-uniform,

$$P_0(R) = n\{1 - 1{\cdot}47\alpha \exp(-\tfrac{3}{4}R^2) + O(\alpha^2)\} \tag{41}$$

and result in an $O(\alpha)$ perturbation determined by

$$\frac{1}{R^2}\frac{d}{dR} R^2 \frac{dg}{dR} - \frac{6g}{R^2} = 2{\cdot}20\alpha R^2 \exp(-\tfrac{3}{4}R^2) \tag{42}$$

with
$$dg/dR = 0 \quad \text{at} \quad R = 0,$$
$$g \to 0 \quad \text{as} \quad R \to \infty,$$

as

$$g(R) = 0{\cdot}98\,\alpha \exp(-\tfrac{3}{4}R^2)\left\{1 + \frac{2}{R^2} - \frac{2}{R^2}\exp(\tfrac{3}{4}R^2)\int_0^R \exp(-\tfrac{3}{4}R^2)\,dR\right\}. \tag{43}$$

The intermolecular particle stress (18) with (35) and (37) and integration over a spherical surface becomes

$$\mathbf{\Sigma}^p_{\mathrm{inter}} = -\tfrac{2}{15}\pi\alpha f_0 N r_g^5 n^2 \mathbf{E} \int_0^\infty R^3 f_{\mathrm{el}}(R)\, P_0(R)\, g(R)\, dR. \tag{44}$$

Completing the integration with (30), (41), and (43) provides

$$\mathbf{\Sigma}^p_{\mathrm{inter}} = 0{\cdot}218\,\alpha^2 f_0 N r_g^5 n^2 \mathbf{E}. \tag{45}$$

As expected the suspension remains Newtonian in the low-shear limit with a small colloidal stress since $\alpha \ll 1$.

Conversely, strong electrostatic repulsion depletes the region $|\mathbf{r}| \lesssim r_g$ of pair space while the uniform distribution persists for $|\mathbf{r}| \gg r_g$. Because of the exponential decay of the electrostatic force law, an abrupt transition between these two limits occurs at the separation characterizing the excluded volume above

$$R^2 \sim \tfrac{4}{3} \ln \alpha.$$

Brownian motion dominates at larger separations, the electrostatic repulsion dominates closer approach and only in the thin intermediate region around $(\frac{4}{3} \ln \alpha)^{\frac{1}{2}}$ must both be considered simultaneously. The leading terms in a matched asymptotic expansion of this form are presented below.

Without diffusion the equation in the inner region, defined by $R \sim O(1)$ reduces to

$$\frac{dg}{dR} = R + O(\alpha^{-1}) \tag{46}$$

with solution

$$g_{\text{inner}} = (c_1 + \tfrac{1}{2}R^2)\,[1 + O(\alpha^{-1})], \tag{47}$$

which satisfies the boundary condition at $R = 0$ (40) despite the singular nature of the expansion in this region.

In the outer region where $R^2 \gg \ln \alpha$ and the electrostatic force can be neglected, the lowest order equation,

$$\frac{1}{R^2}\frac{d}{dR} R^2 \frac{dg}{dR} - \frac{6}{R^2} g = 0 \tag{48}$$

with

$$g \to 0 \quad \text{as} \quad R \to \infty,$$

has solution

$$g_{\text{outer}} = \frac{c_3}{R^3}. \tag{49}$$

In the intermediate region the change of variables

$$R^2 = \tfrac{4}{3} \ln \alpha + \rho \tag{50}$$

balances the Brownian and electrostatic terms as

$$d^2g/d\rho^2 + 1{\cdot}10 \exp(-\tfrac{3}{4}\rho)\, dg/d\rho = 0{\cdot}55 \exp(-\tfrac{3}{4}\rho) + O(dg/d\rho/\ln \alpha). \tag{51}$$

The solution capable of matching the inner and outer solutions is

$$g_{\text{inter}} = c_2 + \tfrac{1}{2}\rho. \tag{52}$$

The correct matching scheme to determine the constants appearing in these three solutions is

$$\begin{aligned} \lim_{R^2 \to \frac{4}{3} \ln \alpha} g_{\text{inner}} &= \lim_{\rho \to -\infty} g_{\text{inter}} \\ \lim_{R^2 \to \frac{4}{3} \ln \alpha} g_{\text{outer}} &= \lim_{\rho \to \infty} g_{\text{inter}}. \end{aligned} \tag{53}$$

As a result

$$c_1 = -\tfrac{10}{9} \ln \alpha, \quad c_2 = -\tfrac{4}{9} \ln \alpha, \quad \text{and} \quad c_3 = -\frac{32}{27\sqrt{3}} (\ln \alpha)^{\frac{3}{2}}. \tag{54}$$

The fact that c_1 and c_2 are not $O(1)$ as implicitly assumed in (47) and (52) is unimportant because the error terms remain $O(\alpha^{-1})$ and $O([\ln \alpha)^{-1}]$, respectively. Figure 3 illustrates the smooth form of the matched solution.

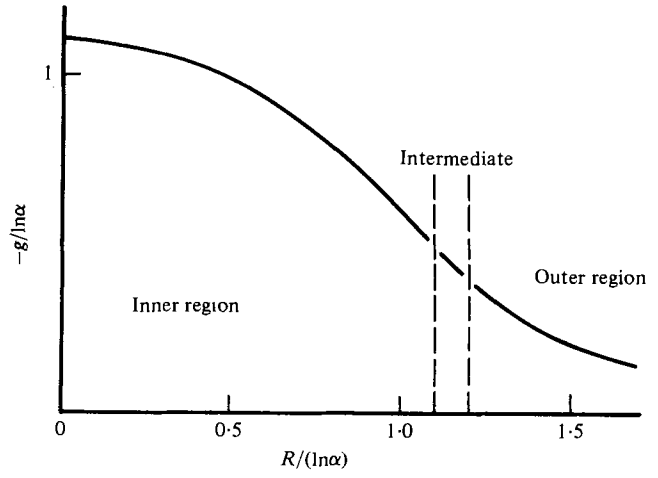

FIGURE 3. Matched asymptotic solution for perturbed pair density $g(R)$ for Gaussian segment density in $\alpha \gg 1$ limit.

The leading contribution to the intermolecular particle stress (44) comes solely from the intermediate region where the integrand is $O(1/\alpha\,(\ln\alpha)^{\frac{5}{2}})$. The inner region contains too few pairs, $P_0 \sim e^{-\alpha}$, while the electrostatic force becomes very weak in the outer, $f_{\rm el} \ll O(\alpha^{-1})$. With the intermediate solution

$$\left.\begin{aligned}\int_0^\infty R^3 f_{\rm el}(R)\,\frac{P_0(R)}{n}\,g(R)\,dR &= -0{\cdot}753\,\frac{(\ln\alpha)^{\frac{5}{2}}}{\alpha}\int_{-\infty}^{\infty}\exp(-\tfrac{3}{4}\rho)\exp(-1{\cdot}47e^{-\frac{3}{4}\rho})\,d\rho\\ &= -0{\cdot}683\,(\ln\alpha)^{\frac{5}{2}}/\alpha\end{aligned}\right\} \tag{55}$$

so that

$$\boldsymbol{\Sigma}^p_{\rm inter} = 0{\cdot}286(\ln\alpha)^{\frac{5}{2}} f_0 N r_g^5 n^2 \mathbf{E}. \tag{56}$$

As α increases the stress also increases without bound. This differs significantly from the following result for a uniform distribution of segments over a fixed volume, an effect of the approximate nature of the Gaussian segment density which never becomes identically zero but permits some overlap even at very large separations. Since the true segment density must be zero at radii greater than half the extended length, this limit becomes suspect for $\frac{4}{3}\ln\alpha \sim \left(\dfrac{Nl}{r_g}\right)^2$.

Uniform segment density

With the electrostatic force law for a uniform segment density the pair conservation equation is amenable to power series solution as well as asymptotic expansions for small and large α. Indeed the three solutions complement one another to cover the full range of α. The analysis differs somewhat from the Gaussian case because the electrostatic force is identically zero for $R > (20/3)^{\frac{1}{2}}$, defining an exterior region in which $P_0 \equiv n$ and $g \propto R^{-3}$. At $R = (20/3)^{\frac{1}{2}}$ both the function and the flux, i.e. derivative, must be continuous indicating that the interior solution must satisfy

$$dg/dR + \tfrac{3}{2}(\tfrac{3}{5})^{\frac{1}{2}} g = 0. \tag{57}$$

For $\alpha \ll 1$ the appropriate interior solutions are

$$P_0 = n\{1 - 1{\cdot}39\alpha[1 - \tfrac{3}{4}(\tfrac{3}{5})^{\frac{1}{2}}(R - \tfrac{1}{20}R^3)]\} \tag{58}$$

and

$$g = 0{\cdot}81\alpha\{-\tfrac{4}{9}(\tfrac{3}{5})^{\frac{1}{2}}R^2 + \tfrac{1}{6}R^3 - \tfrac{1}{160}R^5\} \tag{59}$$

which produces

$$\mathbf{\Sigma}^p_{\text{inter}} = 0{\cdot}232\,\alpha^2 f_0 N r_g^5 n^2 \mathbf{E}. \tag{60}$$

Note that this falls within 10% of the corresponding result for the Gaussian coil.

For $\alpha \gg 1$ the analysis parallels that in the previous section except that the intermediate region now lies just inside $R = (\frac{20}{3})^{\frac{1}{2}}$. Within this boundary layer the rescaled length

$$h = \alpha^{\frac{1}{2}}(1 - \tfrac{3}{20}R^2) \tag{61}$$

reduces (40) to

$$\frac{d^2g}{dh^2} - \left(1{\cdot}04h - \frac{1}{2\alpha^{\frac{1}{2}}}(1 + 1{\cdot}04h^2)\right)\frac{dg}{dh} = 3{\cdot}48\,\frac{h}{\alpha^{\frac{1}{2}}}, \tag{62}$$

with

$$dg/dh = \tfrac{3}{2}g/\alpha^{\frac{1}{2}}$$

at $h = 0$ from (57). The interior and exterior equations are similar to the Gaussian case. The complete solution

$$\left.\begin{aligned} g_{\text{inner}} &= \tfrac{1}{2}R^2 - \frac{50}{9} \\ g_{\text{inter}} &= -\frac{20}{9} - \frac{10}{3\alpha^{\frac{1}{2}}}h \\ g_{\text{outer}} &= -\frac{160}{9}\left(\frac{5}{3}\right)^{\frac{3}{2}}\frac{1}{R^3} \end{aligned}\right\} \tag{63}$$

determines the bulk stress as

$$\mathbf{\Sigma}^p_{\text{inter}} = 15{\cdot}0 f_0 N r_g^5 n^2 \mathbf{E}. \tag{64}$$

This limit is independent of α because the mean separation cannot exceed $2(\frac{20}{3})^{\frac{1}{2}}r_g$, i.e. no interpenetration, regardless of the electrostatic force. Without the next term in the series these two asymptotic limits reflect only crudely the behaviour for $\alpha \approx O(1)$.

For this intermediate range a power series solution has been derived in the form

$$g(r) = r^2 \sum_{n=0}^{\infty} a_n r^n + \tfrac{10}{3}r^2, \tag{65}$$

where $r = (\frac{3}{20})^{\frac{1}{2}}R \leqslant 1$. The recurrence relation

$$a_{n+3} = 2{\cdot}09\alpha\,\frac{(n+2)\,a_n - (n+4)\,a_{n+3}}{(n+8)\,(n+3)} \tag{66}$$

determines the coefficients with

$$a_0 = -50\Big/\left(3\sum_{n=0}^{\infty}\bar{a}_n(n+5)\right), \quad \bar{a}_n = a_n/a_0 \tag{67}$$

following from the boundary condition (57).

With (65) and the expanded equilibrium distribution

$$P_0(r) = n\exp(-1{\cdot}39\alpha)\sum_{k=0}^{\infty}\sum_{m=0}^{\infty}\left(-\frac{1}{3}\right)^m \frac{(2{\cdot}09\alpha)^{k+m}}{m!k!}\,r^{k+3m} \tag{68}$$

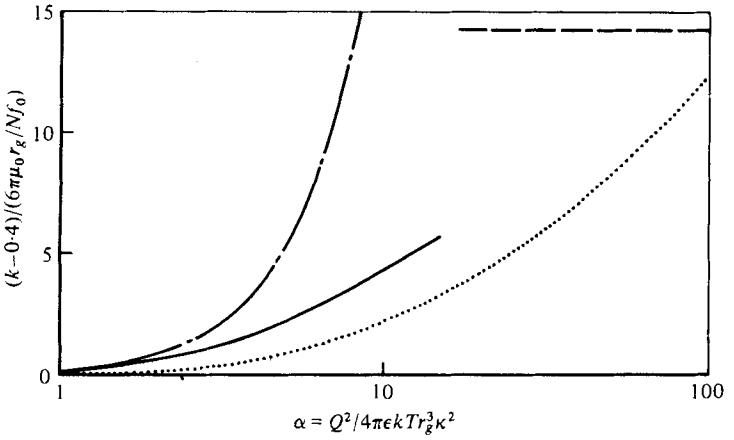

FIGURE 4. Theoretical results for k_{el} including: ——, power series, uniform density; – – –, $\alpha \ll 1$, uniform and Gaussian densities; – – –, $\alpha \gg 1$, uniform density; ·····, $\alpha \gg 1$, Gaussian density.

the particle stress (44) can be integrated analytically as

$$\boldsymbol{\Sigma}^p_{\text{inter}} = 30{\cdot}2\alpha \exp(-1{\cdot}39\alpha) f_0 N r_g^5 n^2 \mathbf{E} \sum_{p=0}^{\infty} \sum_{m=0}^{p} \left(-\frac{1}{3}\right)^{m+1} \frac{(2{\cdot}09\alpha)^p}{m!(p-m)!} \times \left\{ \frac{10}{3} \frac{1}{(p+2m+6)(p+2m+8)} + \sum_{n=0}^{\infty} \frac{a_n}{(p+2m+n+6)(p+2m+n+8)} \right\}. \tag{69}$$

Figure 4 displays the numerical results for $\alpha \leqslant 15$ where the summations become prohibitively time-consuming. The $\alpha \ll 1$ limit coincides with the asymptotic solution and the power series result appears to approach the $\alpha \gg 1$ asymptote.

7. Discussion

In the preceding sections the electrostatic and viscous contributions to the particle stress in the low-shear limit have been derived for Gaussian and uniform segment densities. When added to the solvent contribution these determine the total stress as

$$\boldsymbol{\Sigma} = -(\langle P_0 \rangle + nkT)\boldsymbol{\delta} + 2\mu_0 \mathbf{E}(1 + [\eta]c + [\eta]^2 c^2(\tfrac{2}{5} + k_{el})).$$

The results for the normalized electrostatic component $k_{el}\ 6\pi\mu_0 r_g/Nf_0$ summarized in table 1 and figure 4 demonstrate the insensitivity of the Huggins' coefficient to molecular structure. The uncertainty as to the exact configuration therefore becomes unimportant.

These theoretical predictions have been compared with the data of Pals & Hermans (1952) on dilute solutions of pectin and carboxymethyl cellulose. All relevant parameters were measured independently, i.e. number-averaged molecular weight, radius of gyration, charge, ionic strength, and Huggins' coefficient. The solutions were fractionated but the remaining polydispersity could introduce some uncertainty into $\alpha \propto r_0^{-3}$ since the radii of gyration were calculated from the measured intrinsic viscosities with the free-draining coil result (10). Table 2 illustrates the range of the

Distribution ...	$k_{el}\frac{Nf_0}{6\pi\mu_0 r_g}$	
	$\alpha \ll 1$	$\alpha \gg 1$
Gaussian	$0{\cdot}208\alpha^2$	$0{\cdot}273\ (\ln \alpha)^{\frac{5}{2}}$
Uniform	$0{\cdot}222\alpha^2$	14·3

TABLE 1. Asymptotic results for electrostatic contribution to Huggins' coefficient.

	M_w (10^4)	N	$[\eta]^\infty$ (cm³/g)	r_g^∞ (Å)	Q/e	$\frac{Nf_0}{6\pi\mu_0 r_g^\infty}$	$\frac{Q^2}{\epsilon r_g^\infty kT}$
Pectin	4·6	274	3·81	370	60	0·29	68
Na-CMC 72	6·4	325	3·74	400	141	0·33	345
Na-CMC 74	8·6	391	4·39	440	284	0·35	1280
Na-CMC 73	15·0	725	7·35	600	405	0·48	1900

TABLE 2. Relevant experimental parameters from Pals & Hermans (1952).

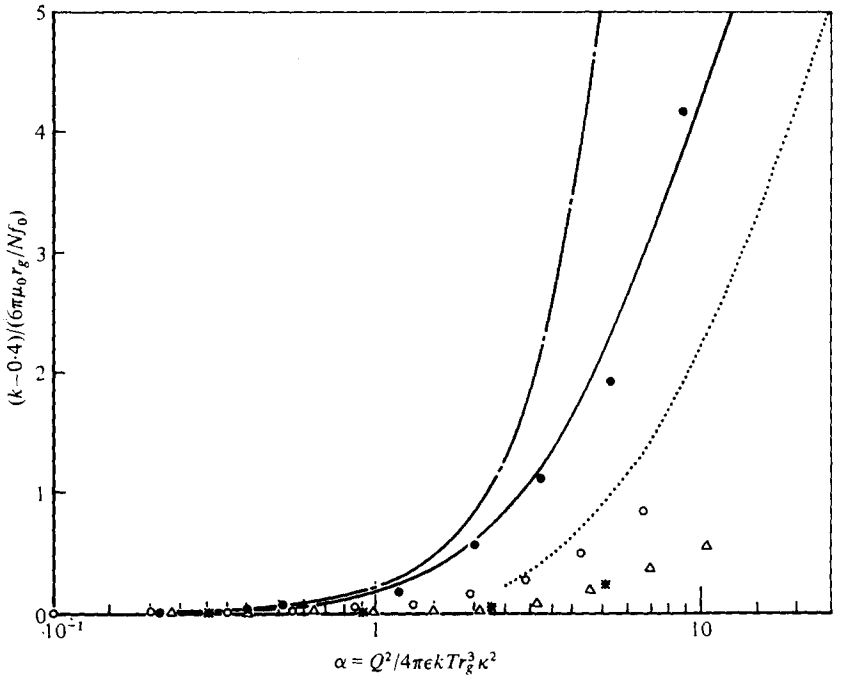

FIGURE 5. Comparison with data of Pals & Hermans (1952). Theoretical curves: ——, power series, uniform density; – – –, $\alpha \ll 1$, Gaussian density; ·····, $\alpha \gg 1$, Gaussian density. Data: ●, pectin $4{\cdot}6 \times 10^4$ M_w; ○, CMC $6{\cdot}4 \times 10^4$ M_w; *, CMC $8{\cdot}6 \times 10^4$ M_w; △, CMC $15{\cdot}0 \times 10^4$ M_w.

relevant experimental parameters. The superscripts ∞ indicate limiting values at high ionic strengths. In all cases the double layers were thin $r_g\kappa < 1$ and the macromolecules were free-draining, $Nf_0/6\pi\mu_0 r_g^\infty \ll 1$; so the experimental conditions conform to the theoretical assumptions.

The superposition of experimental points and theoretical curves in figure 5 reveals good qualitative, but mixed quantitative, agreement. For $\alpha \ll 1$, $k \approx \frac{2}{5}$ as expected from the hydrodynamic interactions while for $\alpha \gtrsim 1$ the Huggins' coefficient certainly increases significantly attaining a maximum value of 21·6 for pectin at the lowest ionic strength. The pectin data falls within the band of theoretical curves but that for carboxymethyl cellulose lies well below. Considering the simplicity of the theory which omits several phenomena (to be discussed below), we feel the agreement to be encouraging.

Intermolecular forces of other than electrostatic origin, such as dispersion forces and hydrogen bonding, generate thermodynamic and mechanical non-idealities in many polymer solutions (Yamakawa 1971). The Flory (1945) and Flory–Krigbaum (1950) theories for solution thermodynamics lump these into an empirical segment–segment interaction parameter $\frac{1}{2}-\chi$ which is zero under ideal conditions. The force laws obtained by integrating over smoothed Gaussian and uniform segment distributions have the same separation dependence as (30) and (31), but with a multiplicative constant proportional to $\frac{1}{2}-\chi$. The theory for the Huggins' coefficient in this paper therefore can be generalized by defining

$$\alpha = \tfrac{1}{3}N^2\frac{V_s^2}{V_0}\frac{\frac{1}{2}-\chi}{\frac{4}{3}\pi r_g^3}$$

to include all relevant forces (V_s = volume of polymer segment, V_0 = volume of solvent molecule) and allowing negative values when attractive forces dominate. Although we have no solutions for $\alpha < 0$ the fact that Pals & Hermans' data for k asymptote to 0·4 as $\alpha \to 0$ (without attractive forces) seems to discount them as the source of the error.

Deformation of the macromolecules from their characteristic equilibrium conformation in dilute solution has also been neglected. Certainly the viscous stresses should be insignificant in the low-shear limit, but intermolecular electrostatic forces could upset the intramolecular balance to alter the conformation. Indeed Yamakawa (1961) demonstrated that in non-electrolyte solutions repulsive pair interactions reduce the average radius of gyration under equilibrium (i.e. no flow) conditions. While this might reduce the Huggins' coefficient in our case, iso-ionic dilution is normally assumed to maintain a concentration-independent conformation for polyelectrolytes (Pals & Hermans 1952).

The most likely explanation for the low experimental values of k for carboxymethyl cellulose is the shear-rate dependence mentioned briefly by Pals & Hermans (1952). As with suspensions of charged spheres (Russel 1978) the electrostatic contribution to the Huggins' coefficient for free-draining macromolecules should be shear-thinning. The effect on this set of data can be gauged by the dimensionless shear rate

$$\Gamma = \frac{Nf_0}{2kT}r_g^2\gamma = \frac{3\mu_0 M_w}{N_A kT}[\eta]\gamma.$$

Although the shear rate γ was constant at 1190 s^{-1} for all runs, Γ varied with the

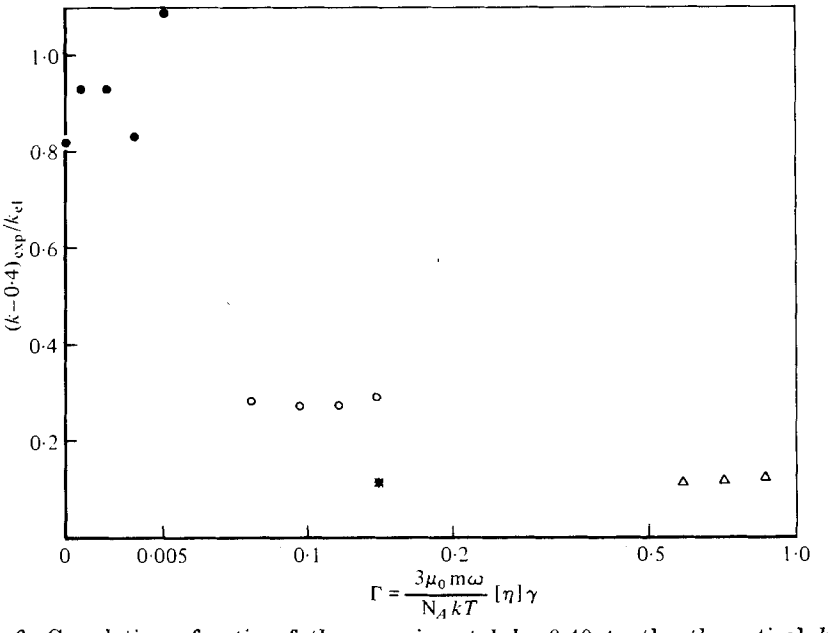

FIGURE 6. Correlation of ratio of the experimental $k-0{\cdot}40$ to the theoretical k_{el} with the dimensionless shear rate: ●, pectin $4{\cdot}6\times10^4\ M_w$; ○, CMC $6{\cdot}4\times10^4\ M_w$; *, CMC $8{\cdot}6\times10^4\ M_w$; △, CMC $15{\cdot}0\times10^4\ M_w$.

molecular weights and ionic strengths of the solutions. In figure 6 the ratio of the measured electrostatic effect to that predicted, i.e. $(k-0{\cdot}40)/k_{el}$, is plotted *vs.* Γ for those runs with $(k-0{\cdot}40)Nf_0/6\pi\mu_0 r_g > 0{\cdot}2$. The overall trend appears to correctly explain the difference between theory and experiment in figure 5 as shear-thinning. The apparently rapid decrease in viscosity at $\Gamma < 0{\cdot}1$ rather than $\Gamma \sim O(1)$ and the lack of supporting trends within the data for each individual polymer remain somewhat troublesome, but the fact that the pectin data which agrees quite well with the predictions falls at the lowest dimensionless shear rate supports the validity of the theory.

In this paper we have drawn two conclusions about the Huggins' coefficient for free-draining macromolecules in weak flows:

(i) in ideal or theta solvents $k = \frac{2}{5}$ as found by Saito (1950) and Felderhof (1976);

(ii) electrostatic repulsions can increase k dramatically above this value.

In both cases the theory predicts an insensitivity to the detailed molecular structure with dependence on only the hydrodynamic parameter $Nf_0/6\pi\mu_0 r_g$ and the dimensionless electrostatic force $\alpha = Q^2/4\pi\epsilon r_g kT(r_g\kappa)^2$. The quantitative predictions agree fairly well with one set of data, but further data on monodisperse polyelectrolytes would be helpful as would attention to several aspects of the theory: the effect of polydispersity, formulation for general intermolecular forces, molecular deformation caused by interaction, and non-Newtonian phenomena in stronger flows.

This work was supported by the National Science Foundation through Grant No. ENG76-04294.

REFERENCES

BAILEY, J. M. 1977 *Macromolecules* **10**, 725.

BATCHELOR, G. K. 1970 *J. Fluid Mech.* **41**, 545.

BATCHELOR, G. K. 1977 *J. Fluid Mech.* **83**, 97.

BATCHELOR, G. K. & GREEN, J. T. 1972 *J. Fluid Mech.* **56**, 375, 401.

BELL, G. M. & LEVINE, S. 1966 *Disc. Far. Soc.* **42**, 69.

BERRY, G. C. 1967 *J. Chem. Phys.* **46**, 1338.

BIRD, R. B., HASSAGER, O., ARMSTRONG, R. C. & CURTISS, C. F. 1977 *Dynamics of Polymeric Liquids: Vol II Kinetic Theory.* John Wiley.

BRINKMAN, H. C. 1947 *Ned. Akad. v. Wet. Amster.* **50**, 618, 821.

DEBYE, P. & BUECHE, A. M. 1948 *J. Chem. Phys.* **16**, 573.

EDWARDS, S. F. 1965 *Proc. Phys. Soc.* **85**, 613.

FELDERHOF, B. U. 1976 *Physica* A **82**, 596, 611.

FIXMAN, M. 1965 *J. Chem. Phys.* **42**, 3831.

FREED, K. F. & EDWARDS, S. F. 1975 *J. Chem. Phys.* **62**, 4032.

FLORY, P. J. 1945 *J. Chem. Phys.* **13**, 453.

FLORY, P. J. & KRIGBAUM, W. R. 1950 *J. Chem. Phys.* **18**, 1086.

DE GENNES, P.-G. 1969 *Rep. Prog. Phys.* **32**, 187.

DE GENNES, P.-G., PINCUS, P. & VELASCO, R. M. 1976 *J. Phys. (Paris)* **37**, 1461.

HERMANS, J. J. & OVERBEEK, J. TH. G. 1948 *Rec. Trav. Chim.* **67**, 761.

KIRKWOOD, J. G. 1934 *J. Chem. Phys.* **2**, 767.

KIRKWOOD, J. G., BUFF, F. P. & GREEN, M. S. 1949 *J. Chem. Phys.* **17**, 988.

KIRKWOOD, J. G. & RISEMAN, J. 1948 *J. Chem. Phys.* **16**, 565.

MANNING, G. S. 1974 In *Polyelectrolytes* (ed. E. Sélégny), pp. 9–37. Reidel.

MOAN, M. & WOLFF, C. 1974 *Die Makrom. Chemie* **175**, 2881.

MUNGAN, N. 1972 *Soc. Petr. Eng. J.* **12**, 469.

PALS, D. T. F. & HERMANS, J. J. 1952 *Rec. Trav. Chim.* **71**, 433.

PETERSON, J. M. & FIXMAN, M. 1963 *J. Chem. Phys.* **39**, 2516.

RICHMOND, P. 1973 *J. Phys.* A **6**, L1C9.

ROUSE, P. E. 1953 *J. Chem. Phys.* **21**, 1272.

RUSSEL, W. B. 1976 *J. Coll. Inter. Sci.* **55**, 590.

RUSSEL, W. B. 1978 *J. Fluid Mech.* **85**, 209.

SAITO, N. 1950 *J. Phys. Soc. Japan* **5**, 4.

SCHOWALTER, W. R. 1978 *Mechanics of Rheologically Complex Fluids.* Pergamon.

WILLIAMS, M. C. 1966 *A.I.Ch.E. J.* **12**, 1064.

WILLIAMS, M. C. 1967 *A.I.Ch.E. J.* **13**, 534.

WILLIAMS, M. C. 1975 *A.I.Ch.E. J.* **21**, 1.

YAMAKAWA, H. 1961 *J. Chem. Phys.* **34**, 1360.

YAMAKAWA, H. 1971 *Modern Theory of Polymer Solutions.* Harper and Row.

ZIMM, B. H. 1956 *J. Chem. Phys.* **24**, 269.